Canadian Conference - Pacific Conference on Earthquake Engineering 2023
Vancouver, British Columbia
June 25th – June 30th, 2023

Effect of Multi-Directional ground motions on the Performance of lead rubber isolators in Base-isolated Bridges

Ashritha Kedarisetti[1*], Carlos E. Ventura[2]

[1]MASc Student, Department of Civil Engineering, University of British Columbia, Vancouver, BC, Canada
[2]Professor, Department of Civil Engineering, University of British Columbia, Vancouver, BC, Canada
[*]settyashi@gmail.com (Corresponding Author)

ABSTRACT

Seismic Isolation is an effective design approach widely used in the seismic design of bridges. Understanding the behaviour of isolation systems and their effects on the overall seismic performance of bridges under different types of ground motions is important. Previous studies reveal the effectiveness of the isolation systems in the presence of vertical ground motion components; however, they have a significant influence on the demands incurred on the isolators. This study explores the impact of multi-directional ground motions on the behaviour of lead rubber isolators in base-isolated bridges. It deals with the axial force demands, hysteresis, and damping behaviour of the isolators which have not been extensively studied in the existing literature.

A 3-span bridge isolated with lead rubber bearings (LRB) is modelled in Seismostruct. A suite of 7 sets of ground motions (GM) is selected for the study. Incremental dynamic analyses of the bridge in the longitudinal direction are carried out with ground motions applied in the longitudinal (L), transverse (T), and vertical (V) directions. The results obtained indicate that axial force demands on the isolators are higher resulting in the demands exceeding the capacities in some analyses. The hysteresis curves generated by dissipating the energy in both horizontal directions of the isolators lead to distorted hysteresis curves. In addition, a great variation in the isolator damping is observed throughout the analyses.

Keywords: Vertical ground motion, Incremental dynamic analysis, Highway bridge, Base isolation, Lead rubber bearing

INTRODUCTION

Base isolation is a system that prevents or at least minimizes the direct and indirect losses of a structure after a seismic event. This concept has gained popularity since the 1970s and is used extensively today due to its effectiveness in protecting structures from earthquake damage. The principle behind base isolation involves separating the superstructure from the ground, reducing the seismic forces transmitted to the superstructure. Base isolation reduces inertial forces developed during an earthquake ground shaking by lengthening the fundamental period of the structure. It can also provide added damping to the structure, further relieving the acceleration demands incurred on the structure.

Seismic isolation in bridges is a particularly widely known application owing to its easy implementation by replacing the expansion bearings in bridges. They are installed between the girders and bent caps (abutments) in bridges. Isolation bearings in bridges have a dual purpose of accommodating thermal expansion and protecting the structure from dynamic loads like earthquake loading. Some of the advantages of base-isolated bridges over fixed-base bridges are decoupling of substructure and superstructure; reduced seismic force demands in substructure; reduced substructure and foundation dimensions; avoiding repair and traffic disruptions after strong earthquakes; overall reduction in the life-cycle cost of the bridge.

Elastomeric and Sliding isolators are widely used base isolators in bridges and have been used in practice since the inception of the seismic isolation concept [1-2] . Since then, significant progress has been made in understanding the behaviour of different isolators and the advantages and disadvantages of using one over the other in bridges when subjected to earthquake ground motions [3-4]. A lot of research has been done to understand the performance of isolators and the influence of isolators on the seismic response of base-isolated bridges in the presence of different types of ground motions [5-9].

In Seismic design, the effect of vertical ground motion components is typically accounted for by increasing the dead load in load combination equations or using two-thirds horizontal spectra. A comparative study of the performance of bridges with and without vertical components done by Button, M.R. et al. [10] revealed that this approach might be too conservative as vertical ground motions significantly affect the seismic response of bridges. Consequently, it was important to understand the behaviour of base-isolated bridges and base isolators when exposed to vertical ground motions.

Over the years, the effect of the vertical seismic component on the performance of isolators in base-isolated bridges has been studied extensively. Warn, G.P. et al. [11] specifically looked into the effects of these ground motions on the response of a bridge isolated with low-damping rubber and lead-rubber isolators using earthquake simulation testing. The study focussed on the contribution of axial load on seismic isolation system and individual bearings due to the vertical component of ground motion. The results from this study suggest that the vertical flexibility of the bridge isolation system should be considered in the design and that relying solely on the peak ground acceleration of the vertical component may underestimate the vertical earthquake load on the isolation system. Rehanogullari, N.E. [12] conducted a comparative study to assess the performance of a 3-span steel composite bridge with and without seismic isolation. The results of this study indicate that the overall performance of the isolated bridge is better than the unisolated bridge. The isolation system increased the girder midspan moment, but the isolator's properties did not significantly impact the midspan girder moment. It is observed that the use of the isolation system decreased the axial force in the presence of vertical ground motions when compared to a fixed base bridge. Landi, L. et al. [13] and Mojidra, R. [14] investigated the influence of vertical ground motions on bridges isolated with sliding bearings.

Shen, J. et al. [5], Diceli, M. [6], and Keramati, A et al. [7] investigated the effect of near-field ground motions on base-isolated bridges. Anajafi, H et al. [8] studied the influence of near-field and far-field ground motions on long-period base-isolated bridges. Marafi, Nasser A., et al. [9] investigated the influence of ground motion duration on the response of bridges isolated with lead rubber bearings, Shape memory alloy rubber bearings (SLRB), and friction pendulum bearings (FPB).

All the past studies concentrated on studying the performance of seismically isolated bridges when compared to fixed base bridges. The literature also indicates that a lot of research has been done to understand the influence of different types of ground motions on the response of isolators and their material properties. However, hysteresis behaviour and damping generated by the isolators when subjected to ground motions in all three directions are not extensively explored. The present study aims to investigate these properties of the isolators by conducting incremental dynamic analyses of a 3-span highway bridge. In addition, the study also sheds light on the axial force demands incurred on the isolators and the consequences of these demands on the isolators and their anchoring systems. It is to be noted that the work presented here is a part of the Master's thesis conducted by the author. [30]

ISOLATOR DESIGN AND BRIDGE MODELLING

Description of the bridge

A three-span highway bridge located at the crossing of Trent River with Highway 19 in Vancouver Island, British Columbia is considered in the study. The bridge was originally designed according to CSA S6-88 (1988) and AASHTO (1992). It is a three-span prestressed concrete bridge with semi-integral abutments. The main span is 40m, with side spans being 33m. The deck of the bridge is made up of three prestressed concrete girders that are 2m thick and are supported by pile caps. The deck slab is a 0.25m thick concrete slab topped with a 0.05m thick asphalt concrete wearing surface. The width of the superstructure is 12m and is fixed at the pier diaphragm pile cap connections. At the abutments, the girders are resting on 600x425x116 mm rubber bearings pads reinforced with five 3 mm thick, grade 300W steel plates. The shear keys facilitate lateral movement of the girders at abutments.

The substructure of the bridge consists of two piers with two circular columns in each pier. Originally, the bridge had two unequal piers. However, in order to avoid the effect of unequal heights of piers on isolator behaviour and purely concentrate on the effects due to ground motion characteristics, it is assumed that the bridge has two piers of equal heights. Each pier of the bridge has a height of 9.83m and is supported by columns with a diameter of 1.5m. The columns have a concrete cover thickness of 75mm. They are reinforced with 28-30M bars arranged longitudinally, resulting in a reinforcement ratio of 1.1%. For transverse reinforcement, 15M spirals are used with a pitch of 0.065m in the plastic hinge region and 0.15m for the rest of the column. The piers have 1.8m deep 6x12.5m concrete spread footings. The specified compressive strength of concrete for all members is 35MPa, and reinforcement grade steel is 400R with a specified yield strength of 400MPa.

The actual bridge consists of east and west bridges, carrying northbound and southbound traffic separately. However, the east bridge is considered as an individual bridge for this study. Detailed illustrations and geometric details of different parts of the bridge are presented in Figure 1.

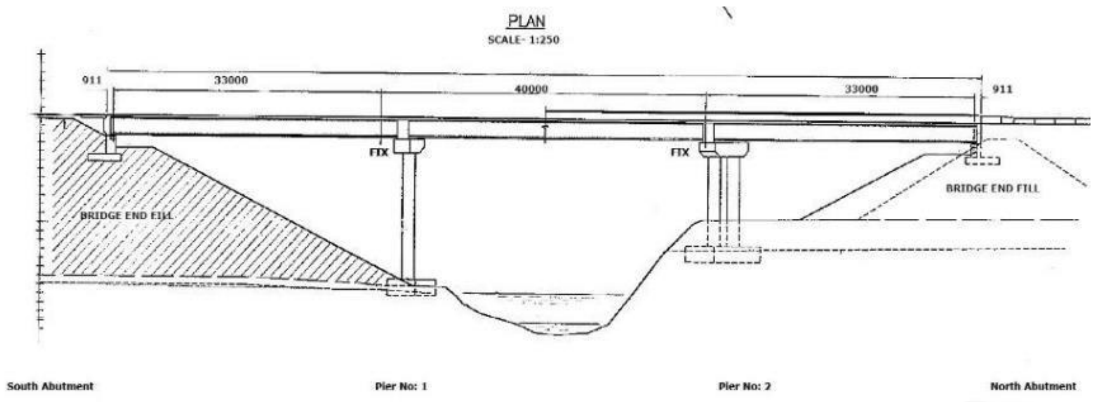

(a)

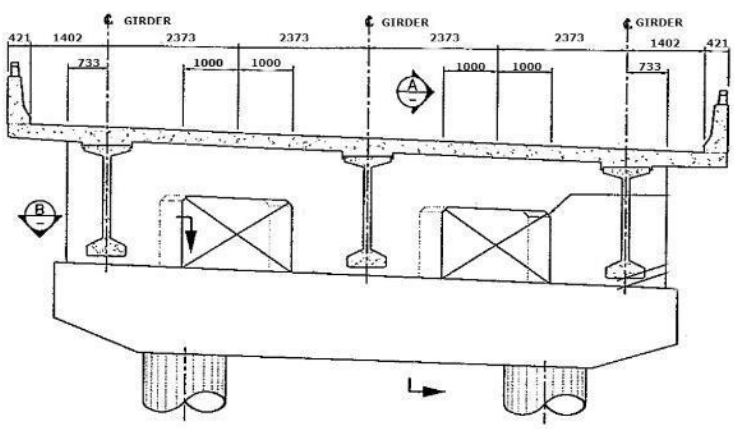

(b)

Figure 1. Details of the bridge: (a) Elevation view (b) Deck details (All dimensions are in mm) [15]

Ground Motion Selection

A suite of ground motions consisting of a mix of long-duration and short-duration ground motions with significant vertical components is selected for the study. The suite consists of seven sets of ground motions from seven earthquakes that are obtained from the NGA West 2 ground motion database [16], Center for Engineering Strong Ground Motion data [17], and Strong-motion Seismograph networks [18]. The list of ground motions used in this study is summarized in Table 1. The location of the bridge assumed in this case study is Vancouver, and the site class considered is Site Class C. The ground motions provided by Natural Resources Canada (NRCAN) [19] for the NBCC 2020 [20] are used to obtain the seismic hazard values of the site (49.25, -123.12) for 2% in 50 years hazard level. The ground motion spectra selected for the study in comparison with the uniform hazard spectrum of the site are illustrated in Figure 2.

Table 1 Ground motions selected

Event	**Magnitude (M_w)**	**Year**	**Station**
Kobe, Japan	6.9	1995	TAZ
Kocaeli, Turkey	7.4	1999	YPT
Duzce, Turkey	7.2	1999	487
Ecuador	7.8	2016	ACHN
Mexico	8.1	1985	SCT1
Peru	8.0	2007	Parcona
Chile	8.8	2010	San Pedro

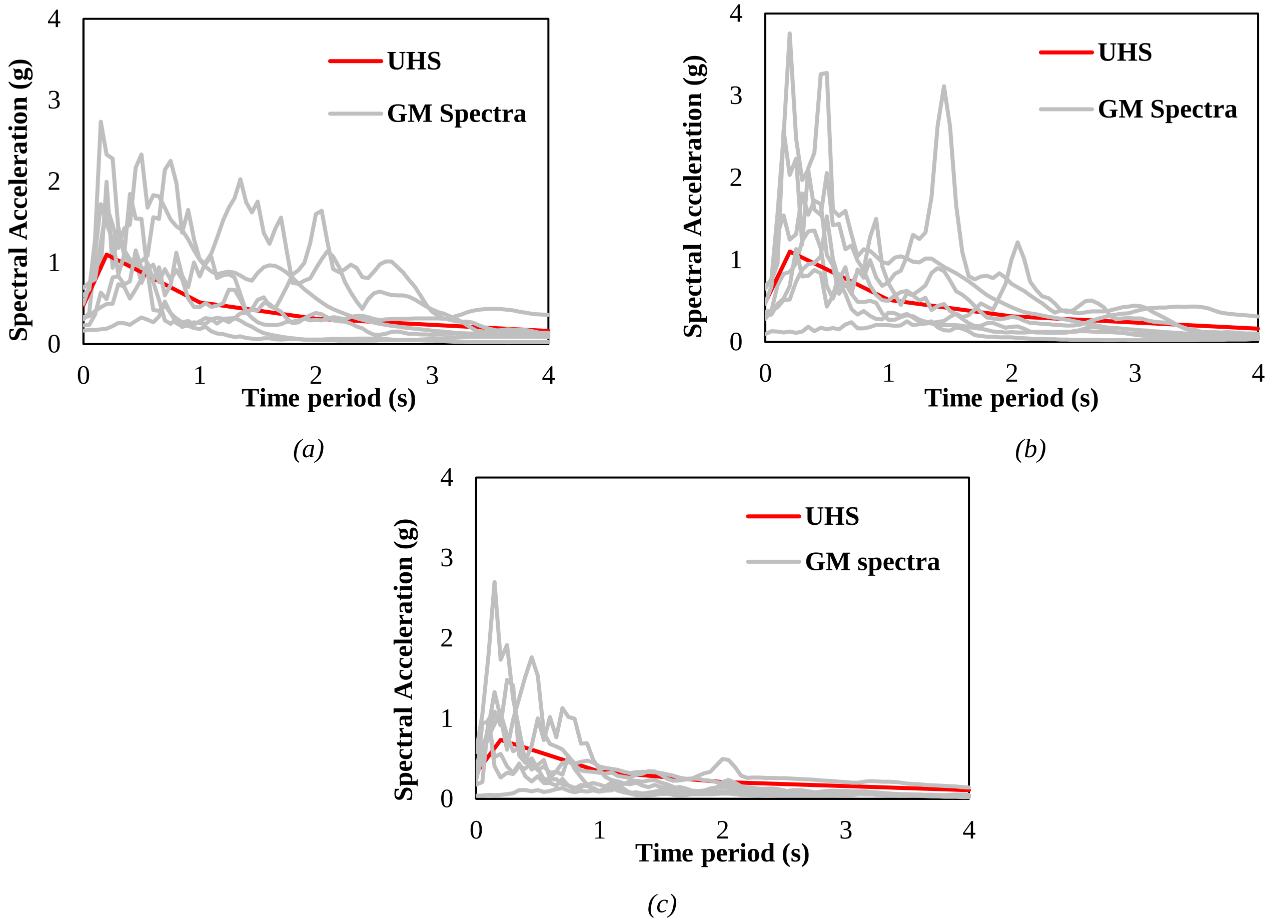

Figure 2 Response spectra: (a) GMs applied in the longitudinal direction (b) GMs applied in the transverse direction (c) GMs applied in the vertical direction

Seismic isolation Bearings

Lead rubber Isolators are considered in this study. The Trent River bridge considered is a fixed base bridge. To conduct the study, lead rubber isolators are designed to convert it into a base-isolated bridge. The isolators are placed in the place of rubber bearings at the abutments and the fixed pier-diaphragm pier cap connections. Therefore, three lead rubber isolators at each pier and abutment are designed using the provisions of the AASHTO Guide Specifications for Seismic Isolation Design [21]. The design procedure outlined in the NHRCP report [22] is used as a reference. The properties of the isolators used in the study are summarized in Table 2.

Table 2 Properties of the lead rubber isolators

Parameter	Unit	Pier Isolator	Abutment Isolator
Characteristic Strength	KN	126.9	254
Post Elastic Stiffness	KN/m	580.1	1164.1
Effective Stiffness	KN/m	2968	1029.9
Axial load capacity	KN	4000	2700
Uplift force	KN	6478.34	2658.98
Maximum deformation	m	0.4	0.4

Finite Element Modelling

A three-dimensional (3D) finite element model of the bridge is developed using a structural analysis program, Seismostruct (Seismosoft 2022) [23]. Figure 3 shows the finite element model of the bridge developed by making some assumptions and idealizations. The superstructure of a base-isolated bridge is assumed to remain elastic under seismic excitation, consistent with the recommendations by Caltrans SDC 1.7. Hence, the girders and the deck are modelled as elastic frame elements (stick model) using equivalent mass and stiffness. The bridge columns are modelled as inelastic displacement-based frame elements with 152 section fibres of confined concrete at the core. The section had confined concrete at the core, unconfined concrete at the cover, and reinforcing steel. A non-linear concrete model, con_ma, that uses the constitutive relationship proposed by Mander et al. [24] is used to model confined and unconfined concrete. Stl_mp, a uniaxial model using Menegetto and Pinto stress-strain relationship, is used to model reinforcing steel. This material model also combines the isotropic hardening measures proposed by Fillipou et al. [25]. The cap beams are modelled as elastic frame elements with rigid connections between the columns and the cap beams. A simplified abutment model is used in this case study. Soil structure interaction at abutments is neglected. In the model, the abutment is replaced with a rigid elastic frame element with a set of translational springs in longitudinal, transverse, and vertical directions. The rigid elastic frame element has a length equal to the width of the deck and El_mat, a simple elastic material model, is used to define the abutment material. The input parameters are the modulus of elasticity and specific weight. A very high modulus of elasticity is chosen to mimic a material that almost acts as a rigid material. In the longitudinal direction, elastic-plastic springs are used. The model uses a hardening ratio that regulates the nature of the curve. In the other directions, linear springs are employed. The stiffness and yield forces of the abutments are obtained from Clause 6.3.1 and Clause 6.3.2 of Caltrans SDC 2019 [26]. Site class C is assumed, and the soil structure interaction of the foundation is neglected. Therefore, the foundations are fixed.

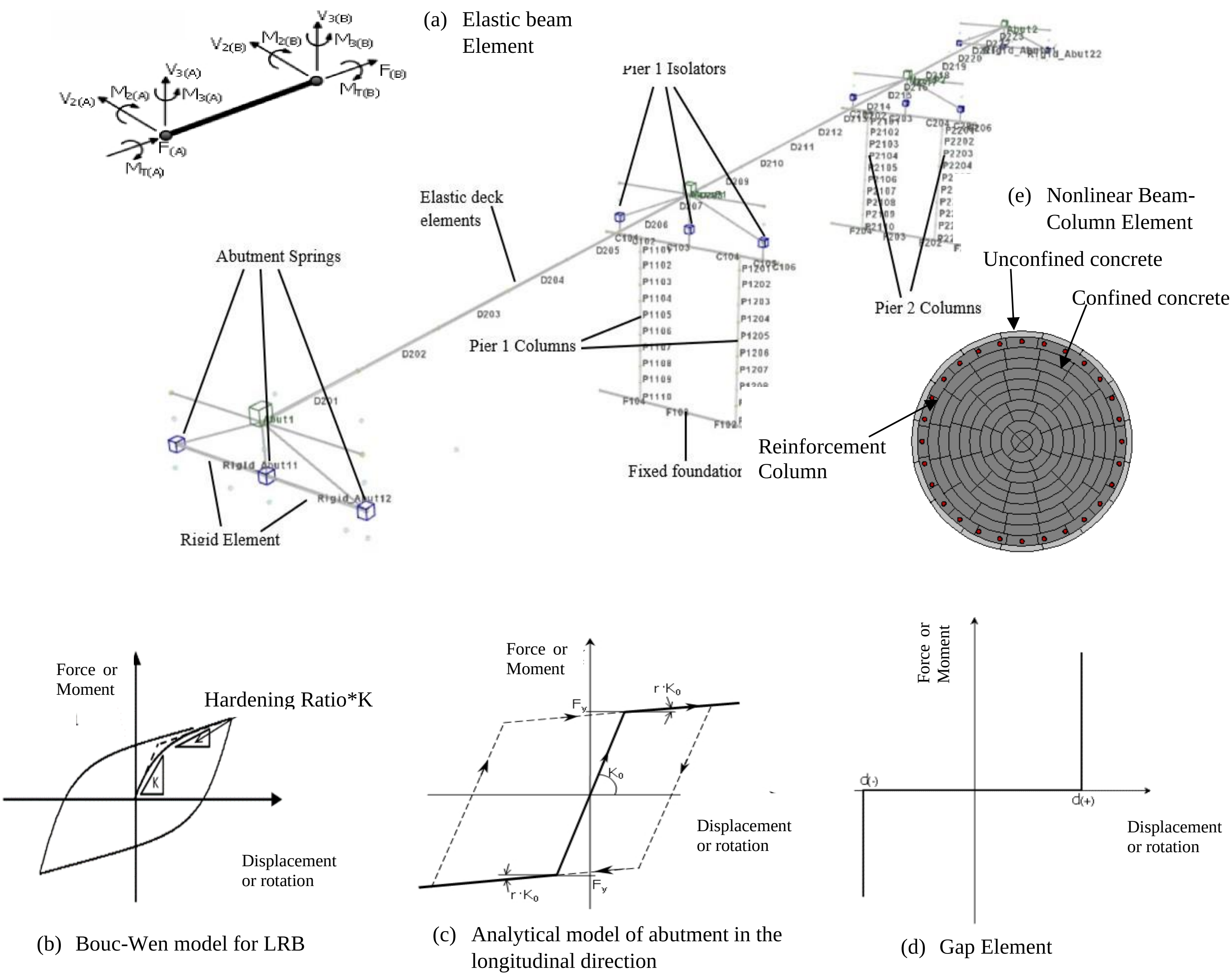

Figure 3 Details of the 3D Model of the bridge: (a) elastic beam element for the superstructure (b) Bouc Wen material model used to model LRB (c) abutment model in longitudinal direction (d) Gap Element (e) Nonlinear Beam-column element used to model columns

A minimum clearance at the ends of the bridge is provided in any isolated bridge to facilitate the displacement of the isolators. In order to model this clearance, a gap element is used. Pounding occurs when the isolator displacement reaches the clearance width. A gap element ensures that there is no resistance until the limit is reached, but as soon as the limit exceeds, it induces very high forces mimicking the pounding in the bridge. The gap_hk model in Seismostruct employed for this very purpose is used here. A link element with gap_hk in both the longitudinal and transverse directions is modelled as a gap element. From the results obtained from the preliminary design and considering a practically possible length of joint cover on the bridge deck to facilitate the isolator movement, a clearance of 0.4m is considered while modelling the gap element.

Lead rubber isolators used in this case study are modelled as an elastomeric bearing link element that implements the hysteresis curve developed by Bouc [27] and Wen [28]. In the bridge model, the isolators are located at the piers and the abutments. The rigid link between the deck and the pier caps is replaced with the isolators at the piers. And at abutments, the expansion joints are replaced with isolators. It is assumed that there is one isolator under each girder. Bearing stiffness in translational directions and bearing characteristic strength values obtained from the design procedure, as shown in Table 2, are used. Estimates of the bearing stiffness in the vertical direction and other rotational orientations were obtained using AS 5100.4-2017. The hardening ratio of 0.1 is used to model the isolators. In Seismostruct, the link elements are modelled as zero-length elements. Two nodes with the same coordinates are created and joined. The element created is known as a zero-length element. This element is now assigned the properties of a link element section in the desired directions. Isolators and gap elements are generated in this manner. The abutments are connected to the gap elements, which are connected to the isolators, which in turn are connected to the deck.

Validation of finite element model

The accuracy of the bearing modelling technique adopted in this case study is checked against the experimental results of lead rubber isolators (LRB) reported by Constantinou et al [29]. The LRB tested under vertical stress of 6.7 MPa under lateral sinusoidal motion with a frequency of 0.35 Hz, and a peak shear strain of 58% was selected. Figure 4 compares the hysteresis behaviour simulated from the model to the experimental results obtained. The comparison shows that the Bouc Wen model can mimic the behaviour of a lead rubber isolator and therefore is reliable to be used in this case study.

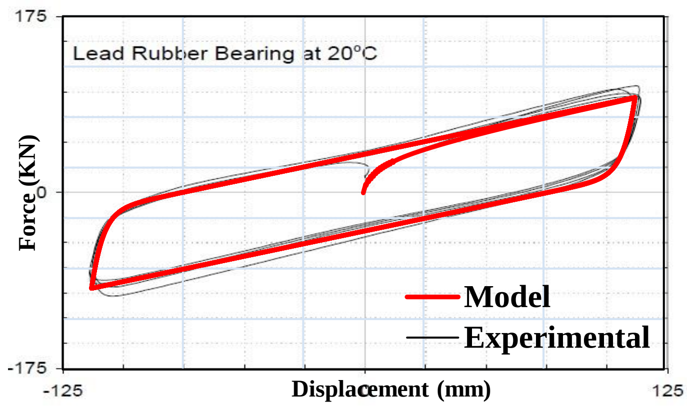

Figure 4 Experimental and Simulated time histories of LRB

Modal Analysis of the isolated bridge

Modal analysis of the bridge is done, and the first four modal periods of the bridge are presented in Table 3. The first mode has a period of 2.583s. The spectral acceleration demand at 2.583s obtained from the UHS considered as shown in Figure 2, is around 0.2g. Thus, the isolation system elongates the period of the structure to 2.583s, where the acceleration demand is significantly lower, thus, fulfilling its purpose.

Table 3 Results obtained from Modal Analysis

Modes	Period (s)	Direction
Mode 1	2.583	Longitudinal
Mode 2	2.484	Transverse
Mode 3	2.322	Torsion
Mode 4	0.453	Vertical

The 3D model created is used to conduct incremental dynamic analysis (IDA) of the bridge. IDA is carried out in the longitudinal direction of the bridge with scaling factors ranging from 1 to 5. In this way, the behaviour of the system under varying ground motion intensities is studied.

RESULTS AND DISCUSSION

The results obtained for a couple of earthquakes out of the seven earthquake ground motions in the suite are presented here. The rest of the results can be found in Ashritha Kedarisetti (2023). [30]

Axial load demands in compression

The results presented in the work done by Ashritha Kedarisetti (2023) [30] indicate that the compressive axial load demand on the isolators is higher when ground motions are applied in both orthogonal and vertical directions. An attempt has been made to understand how these demands would compare to their axial load capacities. The normalized axial force parameter obtained by dividing the compressive axial force demand at the isolator by its capacity is plotted against the scaling factors to get a sense of the demand on the isolator when compared to its capacity and the intensity of the ground motions applied. Figure 5 shows the normalized axial force plots for the sum of axial forces at abutment 1 and pier 1. The results indicate that 57% of the ground motions resulted in axial load demands greater than the capacity of the isolators at abutments in at least one scaling factor of the IDA. For piers, it is 86%. However, it is to be noted that the results presented here are the peak values that typically occur at an instantaneous time. Hence, a closer look is taken at the number of instances and the time for which the axial load capacity of an isolator is exceeded to better understand the effect it would have on the isolators.

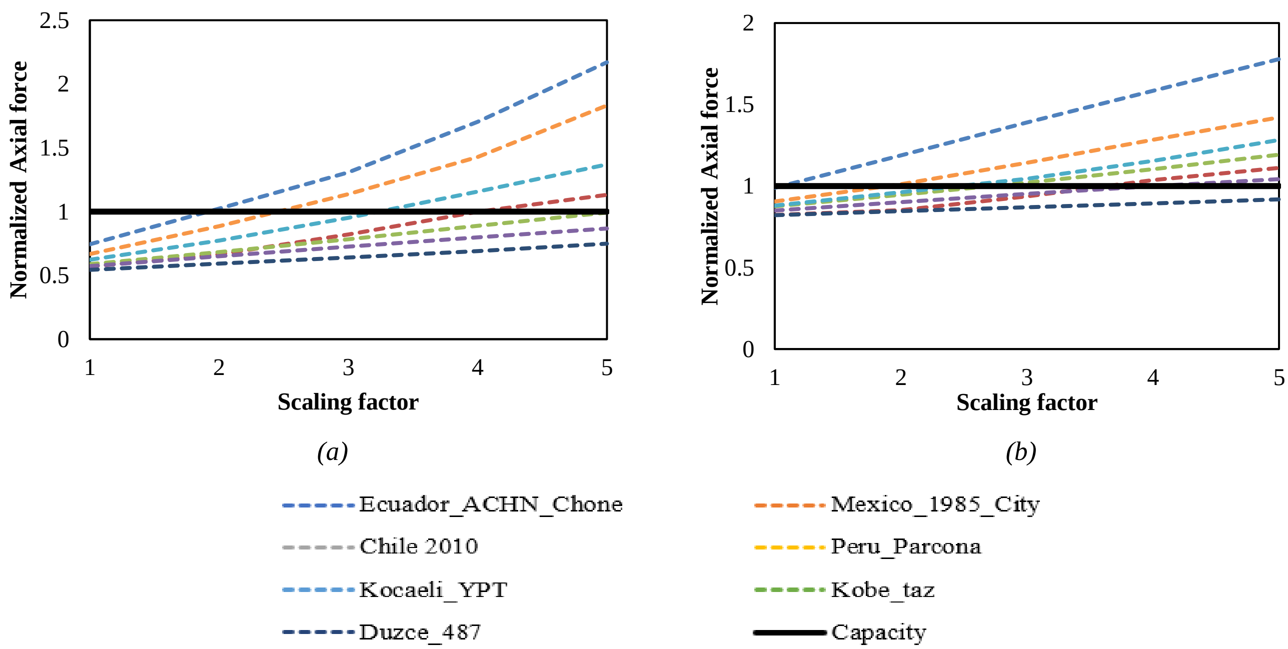

Figure 5 Normalized Axial force Vs Capacity: (a) Abut 1 Isolators (b) Pier 1 Isolators

Table 4 Number of instances and the maximum time for which Axial force demand is greater than the capacity for isolators when Mexico City_1985 and Ecuador_ACHN_Chone ground motions are applied

Axial load demand > Axial load capacity								
Ground Motion	Mexico City_1985				Ecuador_ACHN_Chone			
Time Step (s)	0.02				0.02			
	Abut 1 Isolator		**Pier 1 Isolator**		**Abut 1 Isolator**		**Pier 1 Isolator**	
Scaling factor	**No of instances**	**Max time**	**No of instances**	**Max time**	**No of instances**	**Max time**	**No of instances**	**Max time**
1	0	0	0	0	0	0	0	0
2	0	0	0	0	0	0	8	0.46
3	0	0	0	0	9	0.52	14	0.54
4	2	0.12	2	0.1	11	0.66	17	0.56
5	4	0.6	3	0.14	13	0.62	18	0.58

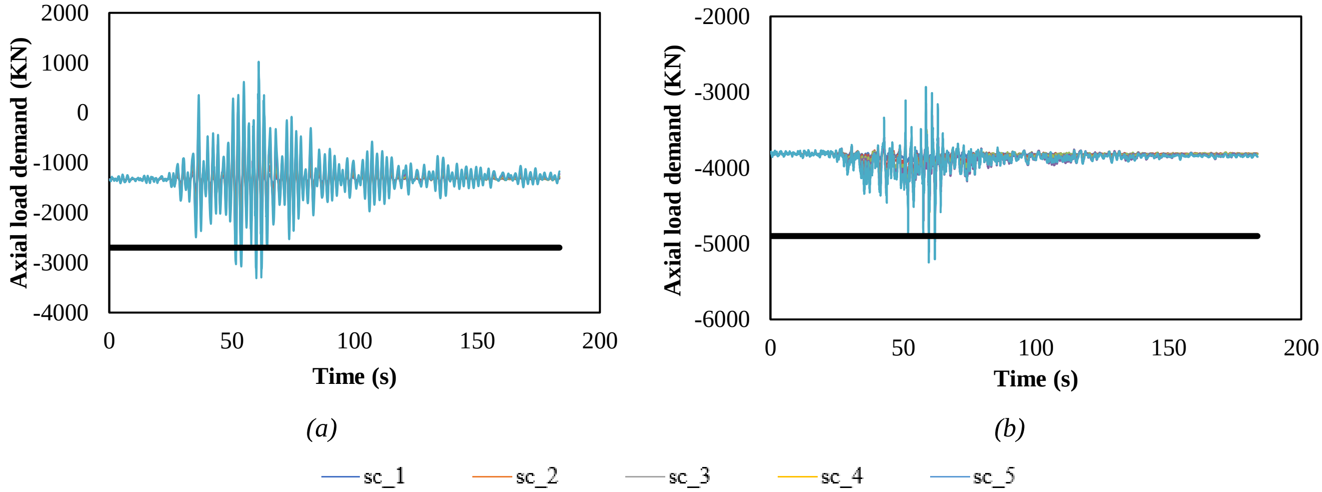

Figure 6 Axial force demands of Isolators when various intensities of Mexico City_1985 ground motions are applied: (a) at abutment 1(b) at Pier 1

Table 4 presents the total number of instances and the maximum amount of time per instance (denoted as max time) when the compressive axial load demand of isolators exceeded their capacity at one of the pier and abutment isolators when the bridge is subjected to Mexico_City_1985 and Ecuador_ACHN_Chone ground motions with varying intensities. Figure 6(a) and Figure 6(b) depict the same graphically for the isolators when Mexico City_1985 ground motion is applied. The results indicate that the number of instances and the amount of time where the axial load demand exceeds capacity varies depending on the characteristics and intensity of the ground motions. It is also observed from the results that the instances where demand exerted on the isolators increased significantly once the isolators reached their deformation capacity. However, further research needs to be done to determine the minimum number of instances or minimum time it would take for the isolators to experience damage when the compressive axial load capacity is exceeded.

Axial load demands in tension

Higher tension axial force demands might result in the failure of the anchoring system causing the isolators to uplift from their positions. Hence, the uplifting force capacity of the anchoring system is compared to the tension demands to check if the isolators are safe. The factored dead and live loads incurred on the isolators multiplied with an uplift factor of 2 gives the uplift force capacity of the anchoring system as shown in Table 2. Since the vertical component of ground motion plays a significant role in the axial force demands, tension force demands incurred on the isolators when subjected to ground motions with a significant vertical component can provide a perspective on the influence of the tension force demands on the anchoring system. The vertical component of Kobe_TAZ ground motion imposes significant demands in the vertical period of the bridge as can be seen in Figure 2 (c). Hence, the isolators' responses to Kobe_TAZ are presented here.

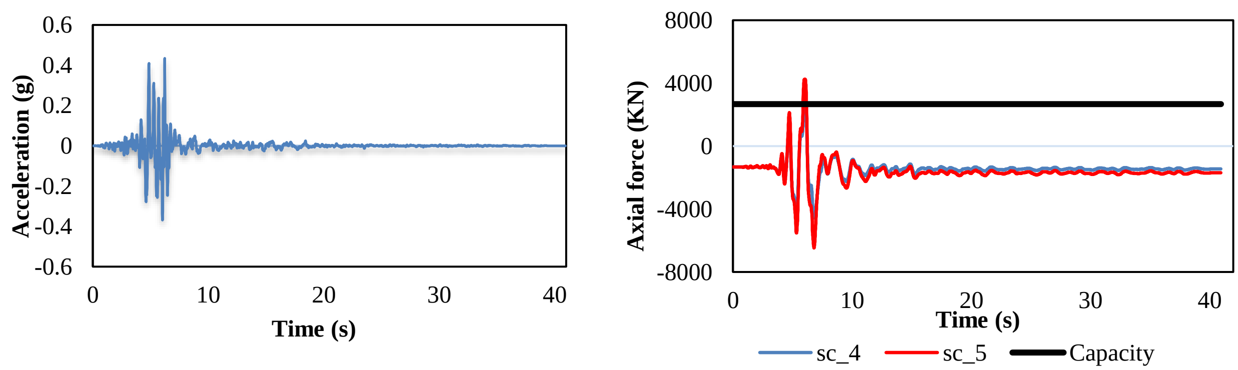

(a) (b)

Figure 7 (a) Acceleration time history data for Kobe_TAZ_Up GM (b) Axial force demands on Abutment isolators when subjected to Kobe_TAZ GM

Figure 7 (a) shows the acceleration time history data of the vertical component of Kobe_TAZ ground motion. The tension force demands on the isolators at abutments exceeded the capacity when the intensity of the ground motion is scaled to a factor of 4 as shown in Figure 7 (b). As stated before, peak values occur at an instantaneous time and are not a good representative to estimate the actual impact on the anchoring system. Therefore, looking into the number of instances and the total time when the tension force demands exceeded the capacity revealed that the tension force demands exceeded the capacity for a maximum of 0.28s (when the intensity of ground motion is scaled to a factor of 5) which is not significant enough to cause the failure of anchorage systems. The axial force demands of the isolators at piers are observed to be well under the capacity of the anchorage systems. From analyzing the results obtained for all the earthquake ground motions in the suite, the tension force demands exceeded the capacity at abutment isolators when the intensities of ground motions are scaled with high scaling factors. It should also be noted that the number of instances this happened remained quite low in all the cases for the isolators to experience damage

Hysteresis Curves

The energy dissipated by the isolators and the resulting hysteresis curves when subjected to ground motions in only one direction and all three directions are compared. Figure 8 shows the hysteresis curves of the abutment isolators in the longitudinal and transverse directions when the Mexico City_1985 ground motion is applied in the L and LTV directions respectively. When ground motion is applied in the longitudinal direction alone, symmetric, and simple hysteresis curves are observed. However, distorted hysteresis curves are observed when the bridge is subjected to translational and vertical ground motions. The isolators dissipating energy in both directions is the reason for this distortion.

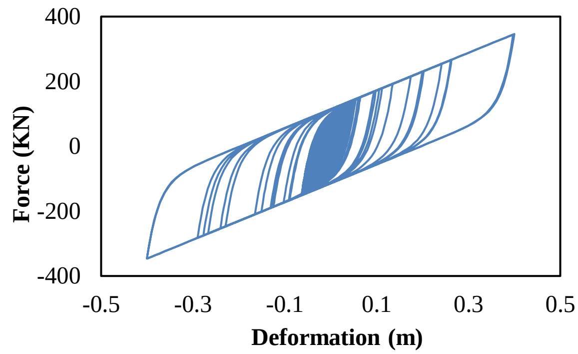

(a)

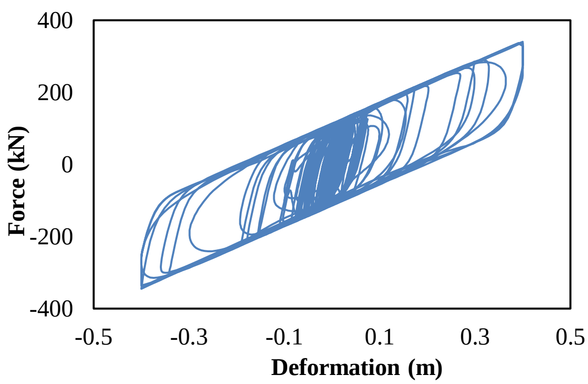

(b)

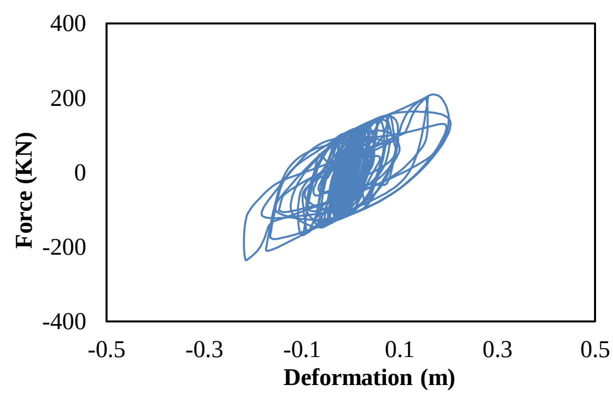

(c)

Figure 8 Hysteresis curves of the abutment isolator in the (a) longitudinal direction when Mexico City_1985 is applied in the L direction (b) longitudinal direction when Mexico City_1985 GM is applied in the L, T, and V directions (c) transverse direction when Mexico City_1985 is applied in the L, T, and V directions

In the modelling of isolators in Seismostruct, the Bouc-Wen model is employed. However, a common way to model lead rubber isolators is to use a bilinear model. When the isolators are modelled using a bilinear relationship and the analyses are carried out, the hysteresis curves obtained resemble textbook-like hysteresis curves. When observed closely, it is evident that the isolators would not result in simpler hysteresis loops. However, when the Bouc-wen model is employed to evaluate the isolators, this difference can be easily seen and understood that a distorted curve is produced when isolators dissipate energy in both directions.

Damping values

Damping produced by the isolators in both horizontal directions when subjected to earthquake excitations in all three directions is calculated using a rudimentary approach here. An area-based approach, proposed by Jacobsen (1960) [31][30] is used here to approximate the damping values of the isolators by equating the energy absorbed by the hysteretic steady-state cyclic response at a given displacement level, as shown in the Eq (1):

$$\xi_{\mathrm{hys}} = \frac{A_h}{2\pi F_m \Delta_m} \tag{1}$$

Where, A_h is the area of the hysteresis loop, F_m and Δ_m are the maximum force and displacement that occurred in the complete cycle. Damping values are computed by selecting hysteretic loops at different intervals during the analysis. This is done to understand the variability of damping provided by the isolators throughout the analysis. This process is applied to hysteresis curves in the longitudinal and transverse directions in all the analyses with scaling factors ranging from 1 to 5. When the intensity of the ground motion applied to the bridge is low, the isolators might be in the elastic range i.e., the deformations are small and there is no significant hysteresis. Damping computations for such cycles of analyses are ignored. The results obtained for Chile_2010 and Mexico City_1995 are shown in Figure 9 and Figure 10.

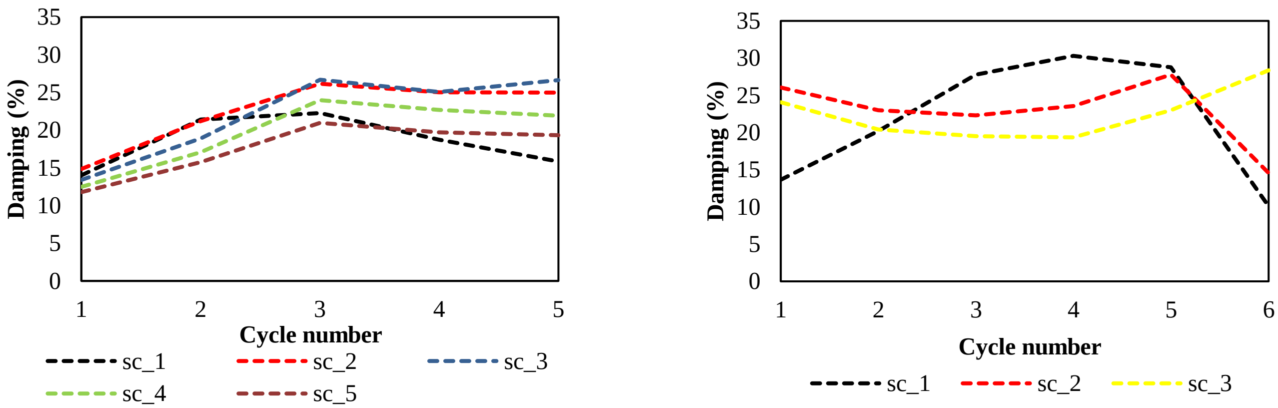

(a) *(b)*

Figure 9 Damping in the longitudinal direction: (a) Chile_2010 (b) Mexico City_1985

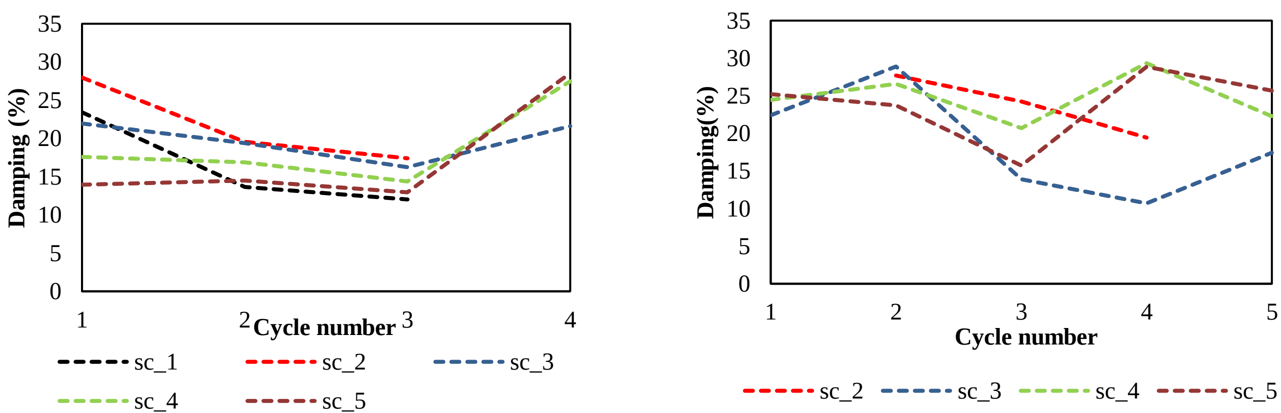

(a) *(b)*

Figure 10 Damping in the transverse direction: (a) Chile_2010 (b) Mexico City_1985

Looking at the above plots and results obtained from calculating damping for the rest of the earthquakes in the suite, it is observed that the damping of the isolators varies significantly. It should be noted, however, that a very rudimentary approach has been used to compute damping in this thesis. Therefore, further study in the area of damping produced by the isolators is recommended.

CONCLUSIONS

The following conclusions can be drawn from this study

- The compressive axial force demands of the isolators when subjected to ground motions in all three directions exceed the axial load capacity of the isolators in some of the analyses. However, the impact it would have on the isolators needs further study.
- The tension axial force demands on the isolators are less than the capacity in most cases. However, even when the demands exceeded the capacity in a few analyses, the time for which it occurred remained quite low. Hence, it can be concluded that the anchoring systems of the isolators are safe against uplift.
- A distorted hysteresis is produced when isolators are subjected to ground motions in all three directions as energy is dissipated in both horizontal directions. Modelling the isolator using the Bouc Wen material model indicated this phenomenon.
- Damping produced by the isolators varied during the analyses, indicating the requirement for an in-depth study to understand the energy-dissipating behaviour of isolators when subjected to ground motions in all three directions.

ACKNOWLEDGMENTS

I would like to thank The University of British Columbia, Vancouver, and the Earthquake Engineering Research Facility (EERF) for providing necessary support throughout the work.

REFERENCES

[1] Buckle, I. G., & Mayes, R. L. (1990). Seismic isolation: history, application, and performance—a world view. *Earthquake Spectra*, *6*(2), 161-201.

[2] Kunde, M. C., & Jangid, R. S. (2003). Seismic behaviour of isolated bridges: A-state-of-the-art review. *Electronic Journal of Structural Engineering*, *3*, 140-170.

[3] Buckle, I., Constantinou, M., Dicleli, M., & Ghasemi, H. (2006). Seismic isolation of highway bridges Kuo, J. (1982). *Fluid-structure interactions: added mass computations for incompressible fluid*. Report No. UCB/EERC-82/09, Earthquake Engineering Research Center, University of California, Berkeley, CA.

[4] Matsagar, V. A., & Jangid, R. S. (2006). Seismic response of simply supported base-isolated bridge with different isolators. *International Journal of Applied Science and Engineering*, *4*(4), 53-69.

[5] Shen, J., Tsai, M. H., Chang, K. C., & Lee, G. C. (2004). Performance of a seismically isolated bridge under near-fault earthquake ground motions. *Journal of Structural Engineering*, *130*(6), 861-868.

[6] Dicleli, M. (2006). Performance of seismic-isolated bridges in relation to near-fault ground motion and isolator characteristics. *Earthquake Spectra*, *22*(4), 887-907.

[7] Keramati, A., & Nouri, G. R. (2020). Effect of behavioural parameters of base isolators on the seismic response of the bridge to near-fault ground motions. *AUT Journal of Civil Engineering*, *4*(3), 277-288.

[8] Anajafi, H., Poursadr, K., Roohi, M., & Santini-Bell, E. (2020). Effectiveness of seismic isolation for long-period structures subject to far-field and near-field excitations. *Frontiers in Built Environment*, *6*, 24.

[9] Marafi, N. A., Eberhard, M. O., Berman, J. W., Wirth, E. A., & Frankel, A. D. (2019). Impacts of simulated M9 Cascadia subduction zone motions on idealized systems. *Earthquake Spectra*, *35*(3), 1261-1287.

[10] Button, M. R., Cronin, C. J., & Mayes, R. L. (2002). Effect of vertical motions on seismic response of highway bridges. *Journal of structural engineering*, *128*(12), 1551-1564.

[11] Warn, G. P., & Whittaker, A. S. (2008). Vertical earthquake loads on seismic isolation systems in bridges. *Journal of structural engineering*, *134*(11), 1696-1704.

[12] Rehanoğulları, N. E. (2010). *Vertical ground motion influence on seismically isolated & unisolated bridges* (Master's thesis, Middle East Technical University).

[13] Landi, L., Grazi, G., & Diotallevi, P. P. (2016). Comparison of different models for friction pendulum isolators in structures subjected to horizontal and vertical ground motions. *Soil Dynamics and Earthquake Engineering*, *81*, 75-83.

[14] Mojidra, R. (2019). Influence of Vertical Ground Motion on Bridges Isolated with Friction Pendulum Bearings (Doctoral dissertation, University of Nevada, Reno).

[15] Design Notes on Trent Bridge provided by Associated Engineering (B.C.) Ltd. (1999)

[16] PEER. (2022). *PEER Ground Motion Database.* available at http://ngawest2.berkeley.edu: Pacific Earthquake Engineering Research Center.

[17] COSMOS. (2008). *Strong-motion Virtual Data Center (VDC).* available at http://www.strongmotioncenter.org: The Consortium of Organizations for Strong-Motion Observation Systems

[18] Fujiwara, H., Aoi, S., Kunugi, T., & Adachi, S. (2004). Strong-motion Observation Networks of NIED: K-NET and KiK-net. *Cosmos Report*.

[19] Natural Resources Canada. (2020). "Determine 2020 National Building Code of Canada seismic hazard values." *https://earthquakescanada.nrcan.gc.ca/hazardalea/interpolat/nbc2020-cnb2020-en.php*
[20] National Research Council of Canada. (2020). *National Building Code of Canada.* Ottawa, Ont.
[21] AASHTO Guide Specifications for Seismic Isolation design (2010).
[22] Buckle, I. G., Al-Ani, M., & Monzon, E. (2011). Seismic isolation design examples of highway bridges. *NCHRP Project*, 20-27.
[23] Seismostruct-Software for Structural Assessment and Structural Retrofitting. *https://seismosoft.com/products/seismostruct/.*
[24] Mander, J. B., Priestley, M. J. N., and Park, R. (1988). "Theoretical Stress-Strain Model for Confined Concrete." *Journal of Structural Engineering,* 114(8), 1804-1826.
[25] Filippou, F. C., Popov, E. P., and Bertero, V. V. (1983). "Effects of Bond Deterioration on Hysteretic Behavior of Reinforced Concrete Joints." *Rep. No. EERC 83-19,* Earthquake Engineering Research Center, University of California, Berkeley.
[26] Caltrans, S. D. C. (2019). Seismic design criteria version 2.0. *Sacramento, CA: State of California, Department of Transportation*.
[27] Bouc, R. (1967). Forced vibrations of mechanical systems with hysteresis. In *Proc. of the Fourth Conference on Nonlinear Oscillations, Prague, 1967*.
[28] Wen, Y. K. (1976). Method for random vibration of hysteretic systems. *Journal of the engineering mechanics division*, *102*(2), 249-263.
[29] Constantinou, M. C., Whittaker, A. S., Kalpakidis, Y., Fenz, D. M., & Warn, G. P. (2007). Performance of seismic isolation hardware under service and seismic loading. *Technical Rep. No. MCEER-07*, *12*.
[30] Ashritha Kedarisetti (2023). Effect of multi-directional ground motions on the behaviour of lead rubber isolators in base-isolated bridges. *University of British Columbia, Vancouver*.
[31] Jacobsen LS (1960) Damping in composite structures. In: Proceedings of 2nd world conference on earthquake engineering, vol 2. Tokyo and Kyoto, Japan, pp 1029–1044